

# Geophysical Research Letters

## RESEARCH LETTER

10.1029/2020GL089649

### Key Points:

- The collisional cooling by background plasma counteracts largely the Landau heating by hiss waves for <50 eV electrons
- The Landau heating can increase the field-aligned fluxes of >50 eV electrons by 1 order of magnitude within 1.5 hr
- Plasmaspheric plume hiss could mediate energy from the ring current electrons through the suprathermal electrons to the ionospheric plasma

### Supporting Information:

- Supporting Information S1

### Correspondence to:

Z. Su and N. Liu,  
szpe@mail.ustc.edu.cn;  
toshpro@mail.ustc.edu.cn

### Citation:

Wang, Z., Su, Z., Liu, N., Dai, G., Zheng, H., Wang, Y., & Wang, S. (2020). Suprathermal electron evolution under the competition between plasmaspheric plume hiss wave heating and collisional cooling. *Geophysical Research Letters*, 47, e2020GL089649. <https://doi.org/10.1029/2020GL089649>

Received 2 JUL 2020

Accepted 6 SEP 2020

Accepted article online 14 SEP 2020

## Suprathermal Electron Evolution Under the Competition Between Plasmaspheric Plume Hiss Wave Heating and Collisional Cooling

**Zhongshan Wang<sup>1,2,3</sup> , Zhenpeng Su<sup>1,2</sup> , Nigang Liu<sup>1,2,3</sup> , Guyue Dai<sup>1,2,3</sup> , Huinan Zheng<sup>1,2</sup> , Yuming Wang<sup>1,2</sup> , and Shui Wang<sup>1,2</sup>**

<sup>1</sup>Department of Geophysics and Planetary Sciences, University of Science and Technology of China, Hefei, China,

<sup>2</sup>CAS Center for Excellence in Comparative Planetology, University of Science and Technology of China, Hefei, China,

<sup>3</sup>Anhui Mengcheng Geophysics National Observation and Research Station, University of Science and Technology of China, Mengcheng, China

**Abstract** Suprathermal electrons are a major heat source of ionospheric plasma. How the suprathermal electrons evolve during their bounces inside the plasmasphere is a fundamental question for the magnetosphere-ionosphere coupling. On the basis of Van Allen Probes observations and quasi-linear simulations, we present here the first quantitative study on the evolution of suprathermal electrons under the competition between Landau heating by whistler mode hiss waves and Coulomb collisional cooling by background plasma inside a plasmaspheric plume. We show that the Landau heating can prevail over the collisional cooling for >50 eV electrons and cause the field-aligned suprathermal electron fluxes to increase by up to 1 order of magnitude within 1.5 hr. Our results imply that the plasmaspheric plume hiss waves could mediate energy from the ring current electrons to the ionospheric plasma.

**Plain Language Summary** The ionospheric plasma temperature variation can affect the Earth's atmospheric escape and the spacecraft orbit decay. A major heat source of the ionospheric plasma is the suprathermal (several eV to hundreds of eV) electrons, which can bounce along the magnetic field lines inside the plasmasphere. How these suprathermal electrons evolve during their bounces is a fundamental question for the magnetosphere-ionosphere coupling. In the past, the plasmaspheric suprathermal electrons were usually considered to gain energy from the ring current ions through Coulomb collisions and wave-particle interactions. Here we show that strong whistler mode hiss waves can grow from the instability of the ring current electrons in the plasmaspheric drainage plume, and their Landau heating can prevail over the collisional cooling by background plasma for >50 eV electrons. The enhanced field-aligned suprathermal electrons could eventually heat the ionospheric plasma. These results have significant implications for understanding the energy transfer process from the magnetosphere to the ionosphere.

## 1. Introduction

The suprathermal (several eV to hundreds of eV) electrons can effectively heat the ionospheric plasma via both elastic and inelastic collisions (Lemaire & Gringauz, 1998). They are produced from the ionization of atmospheric neutral particles by solar extreme ultraviolet photons and by magnetospheric energetic particles (Schunk & Nagy, 2009). These suprathermal electrons can escape from the production region and bounce along the geomagnetic field lines in the plasmasphere (Hanson, 1964). How the plasmaspheric suprathermal electrons evolve is a fundamental question in the magnetosphere-ionosphere coupling (Khazanov & Liemohn, 1995; Khazanov et al., 1992).

During geomagnetically active times, the plasmaspheric suprathermal electrons are envisioned to conduct the heat flux from the ring current ions to the ionospheric thermal plasma (Brace et al., 1988; Foster et al., 1994; Green et al., 1986; Horwitz et al., 1986). Two leading physical processes have been proposed for such energy transfer. One is the classical Coulomb collisional scattering of the plasmaspheric suprathermal electrons by the ring current ions (e.g., Cole, 1965; Fok et al., 1991; Jordanova et al., 1996; Kozyra et al., 1987; Liemohn et al., 2000). The other is the Landau heating of the plasmaspheric suprathermal electrons by the electromagnetic ion cyclotron waves growing from instabilities of the ring current ions (e.g., Cornwall

et al., 1971; Erlandson et al., 1993; Gurgiolo et al., 2005; Hasegawa & Mima, 1978; Horne & Thorne, 1993; Thorne & Horne, 1992; Yuan et al., 2014; Zhou et al., 2013). In contrast, little attention has been paid to the possible energy transfer between the ring current electrons and the plasmaspheric suprathermal electrons. Whistler mode hiss waves can be excited by the ring current electrons in the plasmasphere (Meredith et al., 2018; Omura et al., 2015; Summers et al., 2014; Su et al., 2018a, 2018b; Thorne et al., 1979), and these waves are expected to subsequently transfer part of their energy to the plasmaspheric suprathermal electrons through the Landau resonance (e.g., Bortnik et al., 2008; Chen et al., 2009). This expected process was seemingly supported by an observation of the field-aligned suprathermal electron flux enhancement associated with the whistler-mode waves inside a remnant plasmaspheric plume (Woodroffe et al., 2017). Subsequently, a quasi-linear simulation (Li et al., 2019) roughly reproduced the field-aligned heating of suprathermal electrons by the Landau resonance with hiss waves in a plasmaspheric plume. However, an important cooling mechanism for suprathermal electrons (Khazanov & Liemohn, 1995), Coulomb collisions with the background plasma, has not been taken into account in the previous studies (Li et al., 2019; Woodroffe et al., 2017).

In this letter, we quantitatively investigate the competition between hiss-driven Landau heating and Coulomb collisional cooling in the evolution of plasmaspheric suprathermal electrons. Using Van Allen Probes observations and quasi-linear simulations, we determine the favored conditions for the transfer of energy from ring current electrons through field-aligned suprathermal electrons to ionospheric plasma. These results have significant implications for understanding the magnetosphere-ionosphere coupling.

## 2. Van Allen Probes Observations

On 30 January 2014, Van Allen Probe B passed a series of finger-like plasmaspheric plumes and observed the energy transfer among electrons of different energies (Figure 1). The Electric and Magnetic Field Instrument and Integrated Science (EMFISIS) suite (Kletzing et al., 2013) and the Energetic Particle, Composition, and Thermal Plasma (ECT) suite (Spence et al., 2013) provided data for our analysis. The Helium Oxygen Proton Electron (HOPE) Mass Spectrometer (Funsten et al., 2013) and the Magnetic Electron Ion Spectrometer (MagEIS) (Blake et al., 2013) of the ECT suite measured the electron differential flux  $j$  as a function of the local pitch angle  $\alpha$  and the kinetic energy  $E_k$ . With the wave spectral matrix from the waveform receiver (WFR) of the EMFISIS Waves instrument, we can calculate the total magnetic power density  $P_B$ , the normal angle  $\psi_B$  (Santolík et al., 2002, 2003), and the sign of field-aligned Poynting flux  $S_B$  (Santolík et al., 2010). With the upper hybrid resonance frequency from the high frequency receiver (HFR) of the EMFISIS Waves instrument, we can derive the local cold electron density  $N_e$  (Kurth et al., 2014). The triaxial fluxgate magnetometer of the EMFISIS suite measured the local magnetic field  $B_0$ . Along a magnetic field line, we assume that the magnetic field strength scaled with the TS04 geomagnetic field model (Tsyganenko & Sitnov, 2005).

A moderate substorm occurred around 02:50 UT as identified by the increase of AE index. Approximately 40 min later, Van Allen Probe B encountered the substorm injection of electrons with energies up to 100 keV and received the strong whistler mode hiss waves with amplitudes up to 0.3 nT in the plasmaspheric plumes. These plume hiss waves propagated mainly in the anti-field-aligned direction away from the equator, consistent with previous observations (Shi et al., 2019; Su et al., 2018a; Woodroffe et al., 2017; Zhang et al., 2019). As discussed by Su et al. (2018a), these waves could be a result of the combined linear and nonlinear instabilities of the freshly injected ring current electrons (Omura et al., 2015; Summers et al., 2014; Thorne et al., 1979). Corresponding to the intense plume hiss waves (e.g., TR<sub>1</sub> and TR<sub>2</sub>), there were significant enhancements in the field-aligned suprathermal electron fluxes at energies 50–300 eV. In contrast, no flux enhancements were observable in the absence of strong hiss waves near the plume boundary (TR<sub>0</sub>). These observations imply the link between plume hiss waves and the suprathermal electron heating. However, after 06:30 UT, Van Allen Probe B went into the plasmaspheric body but observed no enhancement of field-aligned suprathermal electron fluxes (TR<sub>3</sub>). Compared to plume hiss waves, the hiss waves in the plasmaspheric body had ~5 times smaller amplitudes but much larger normal angles. The larger normal angles the waves have, the stronger damping the waves should experience. In addition, according to previous statistical studies (e.g., Agapitov et al., 2018; Li et al., 2015; Meredith et al., 2004; Summers et al., 2008; Tsurutani et al., 2015), the hiss waves in the plasmaspheric body should persist over a longer time than those in the plume. A question arises as to why the significant heating of suprathermal electrons tend to occur in the plasmaspheric plumes rather than in the plasmaspheric body.

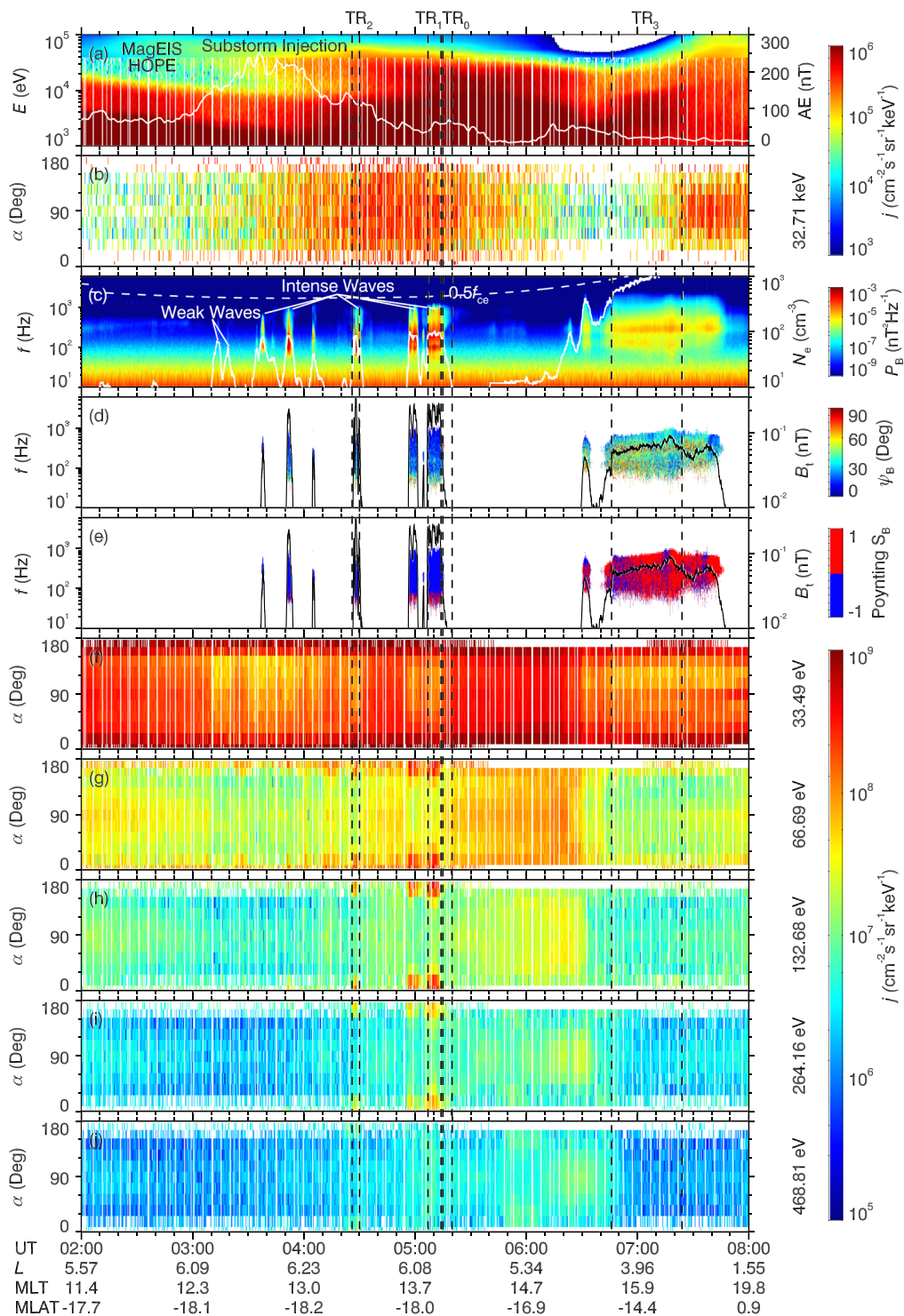


**Figure 1.** Overview of magnetosospheric environment observed by Van Allen Probe B on 30 January 2014: (a) energy-dependent omnidirectional differential fluxes  $j$  of the ring current electrons (color coded), with the overplotted line for the geomagnetic index AE; (b) pitch angle-dependent differential fluxes  $j$  of electrons at energy 32.71 keV (color coded); (c) wave magnetic power spectral densities  $P_B$  (color coded), with the overplotted lines for half the equatorial electron gyrofrequency  $0.5 f_{ce}$  (dashed) and the ambient cold electron densities  $N_e$  (solid); (d, e) wave normal angles  $\psi_B$  and Poynting flux signs  $S_B$  (color coded), with the overplotted lines for the whistler mode wave amplitude  $B_t$ ; (f-j) pitch angle-dependent differential fluxes  $j$  of suprathermal electrons (color coded) at energies 33.49, 66.69, 132.68, 264.16, and 468.81 eV, respectively. The vertical dashed lines mark four time intervals of interest:  $TR_0$  (05:15–05:20 UT),  $TR_1$  (05:07–05:14 UT),  $TR_2$  (04:26–04:30 UT), and  $TR_3$  (06:46–07:24 UT).

### 3. Quasi-Linear Simulations

#### 3.1. Numerical Model

We use the two-dimensional STEERB model (Su et al., 2010; Xiao et al., 2009) to simulate the electron evolution during the TR<sub>1</sub> period from 05:07 UT to 05:14 UT where the most significant enhancement in the field-aligned electron fluxes occurred (Figure 1). The basic equation is the bounce-averaged Fokker-Planck equation (Jordanova et al., 1996; Lyons & Williams, 1984; Schulz & Lanzerotti, 1974)

$$\frac{\partial F}{\partial t} = \frac{1}{G} \frac{\partial}{\partial \alpha_{\text{eq}}} \left[ G \left( \langle D_{\alpha_{\text{eq}} \alpha_{\text{eq}}}^{\text{wp}} \rangle + \langle D_{\alpha_{\text{eq}} \alpha_{\text{eq}}}^{\text{cc}} \rangle \right) \frac{\partial F}{\partial \alpha_{\text{eq}}} + \langle D_{\alpha_{\text{eq}} p}^{\text{wp}} \rangle \frac{\partial F}{\partial p} \right] + \frac{1}{G} \frac{\partial}{\partial p} \left[ G \left( \langle D_{\alpha_{\text{eq}} p}^{\text{wp}} \rangle \frac{\partial F}{\partial \alpha_{\text{eq}}} + \langle D_{pp}^{\text{wp}} \rangle \frac{\partial F}{\partial p} \right) \right] + \frac{1}{G} \frac{\partial}{\partial p} \left( G A_p^{\text{cc}} f \right), \quad (1)$$

with

$$G = p^2 T_{(\alpha_{\text{eq}})} \sin \alpha_{\text{eq}} \cos \alpha_{\text{eq}}, \quad (2)$$

$$T(\alpha_{\text{eq}}) \approx 1.30 - 0.56 \sin \alpha_{\text{eq}}. \quad (3)$$

Here  $F = j/p^2$  is the electron phase space density depending on the equatorial pitch angle  $\alpha_{\text{eq}}$  and the momentum  $p$ , and  $\langle D \rangle$  and  $\langle A \rangle$  are the diffusion and advection coefficients, with the subscripts representing the physical dimensions for transport and the superscripts “wp” and “cc” denoting wave-particle interactions and Coulomb collisions. The computational domain is set to  $\alpha_{\text{eq}} \in [0^\circ, 90^\circ] \times E_k \in [1 \text{ eV}, 1 \text{ keV}]$ . At  $E_k = 1 \text{ eV}$  without resonances (Figure 2), the fixed boundary condition  $\partial f / \partial t = 0$  is applied. At  $E_k = 1 \text{ keV}$ , the fixed boundary condition  $\partial f / \partial t = 0$  is adopted to simulate the balance between the drift and the local resonances. At  $\alpha_{\text{eq}} = 90^\circ$ , the boundary condition  $\partial f / \partial \alpha_{\text{eq}} = 0$  is utilized to characterize the symmetry of the plasmaspheric electron distribution. At  $\alpha_{\text{eq}} = 0^\circ$ , the boundary condition  $\partial f / \partial \alpha_{\text{eq}} = 0$  is expediently used to allow the heating of the field-aligned suprathermal electrons. Considering that the ionosphere is a source of the suprathermal electrons, we artificially set  $F(t, \alpha_{\text{eq}}, p) = \text{Max} \{F(t, \alpha_{\text{eq}}, p), F(0, \alpha_{\text{eq}}, p)\}$  inside the loss cone.

We follow the procedure of Albert (2010) to calculate the bounce-averaged diffusion coefficients of the plasmaspheric plume hiss waves at the magnetic shell  $L = 6.02$ . As plotted in Figure S1 of supporting information, we have validated this quasi-linear diffusion coefficient code against our previously developed test-particle code (Su et al., 2014) for a small-amplitude monochromatic whistler wave using the technique proposed by Liu et al. (2010), Tao et al. (2011), and Su et al. (2012). According to the observations in Figure 1, the background magnetic field is set to a dipole with the equatorial magnetic field  $B_{\text{eq}} = 134 \text{ nT}$ . The field-aligned cold electron density is modeled as (Denton et al., 2002)

$$N_e = N_{\text{eq}} \cos^{-2\nu} \lambda, \quad (4)$$

with the latitudinal variation index  $\nu = 1.5$  given by Denton et al. (2002) at  $L = 6.02$  and the equatorial density  $N_{\text{eq}} = 78 \text{ cm}^{-3}$  derived from the measurements at latitude  $\lambda \approx -18^\circ$  (Figure 1c). The time-averaged magnetic power spectra  $P_B$  is fitted to a piecewise function (Figure 2a), and each piece is a Gaussian function (Lyons & Thorne, 1972). Their specific fitting parameters are as follows: wave amplitudes  $B_t = \{0.073, 0.126, 0.108, 0.072\} \text{ nT}$ , central frequencies  $f_m/f_{ce} = \{0.015, 0.036, -0.038, 0.166\}$ , half-widths  $f_d/f_{ce} = \{0.004, 0.012, 0.072, 0.087\}$ , lower cutoffs  $f_l/f_{ce} = \{0.007, 0.019, 0.046, 0.112\}$ , and upper cutoffs  $f_u/f_{ce} = \{0.019, 0.046, 0.112, 0.378\}$ . Following early studies (e.g., Horne et al., 2005; Meredith et al., 2007; Ni et al., 2014), the tangent of wave normal angle  $\tan \psi_B$  is simply assumed to vary as a Gaussian function with a center  $X_m = 0$ , a half-width  $X_\omega = \tan 20^\circ$ , a lower cutoff  $X_1 = 0$  and an upper cutoff  $X_2 = 1$ . All four wave pieces ( $0.007f_{ce} < f < 0.378f_{ce}$ ) are assumed to occur in the latitude range  $|\lambda| < 40^\circ$  (Li et al., 2015; Meredith et al., 2018). As shown in Figures 2b, 2e, 2h, and 2k, the cyclotron resonance is limited to be above 300 eV and the Landau resonance extends down to 5 eV. The peak diffusion rates  $\langle D_{pp}^{\text{wp}} \rangle / p^2$  reach  $5 \times 10^{-5} \text{ s}^{-1}$  near the loss cone, implying the substantial wave-driven evolution of electrons on a time scale of several hours.

Following the work of Jordanova et al. (1996), we calculate the bounce-averaged diffusion and advection coefficients related to the Coulomb collisions with the background cold electrons. The Coulomb collisional transport related to the cold ions is negligible in comparison to that related to the cold electrons (Khazanov et al., 1996). In the calculation, the cold electron temperature is assumed to be  $T_e = 1 \text{ eV}$ , and the ambient

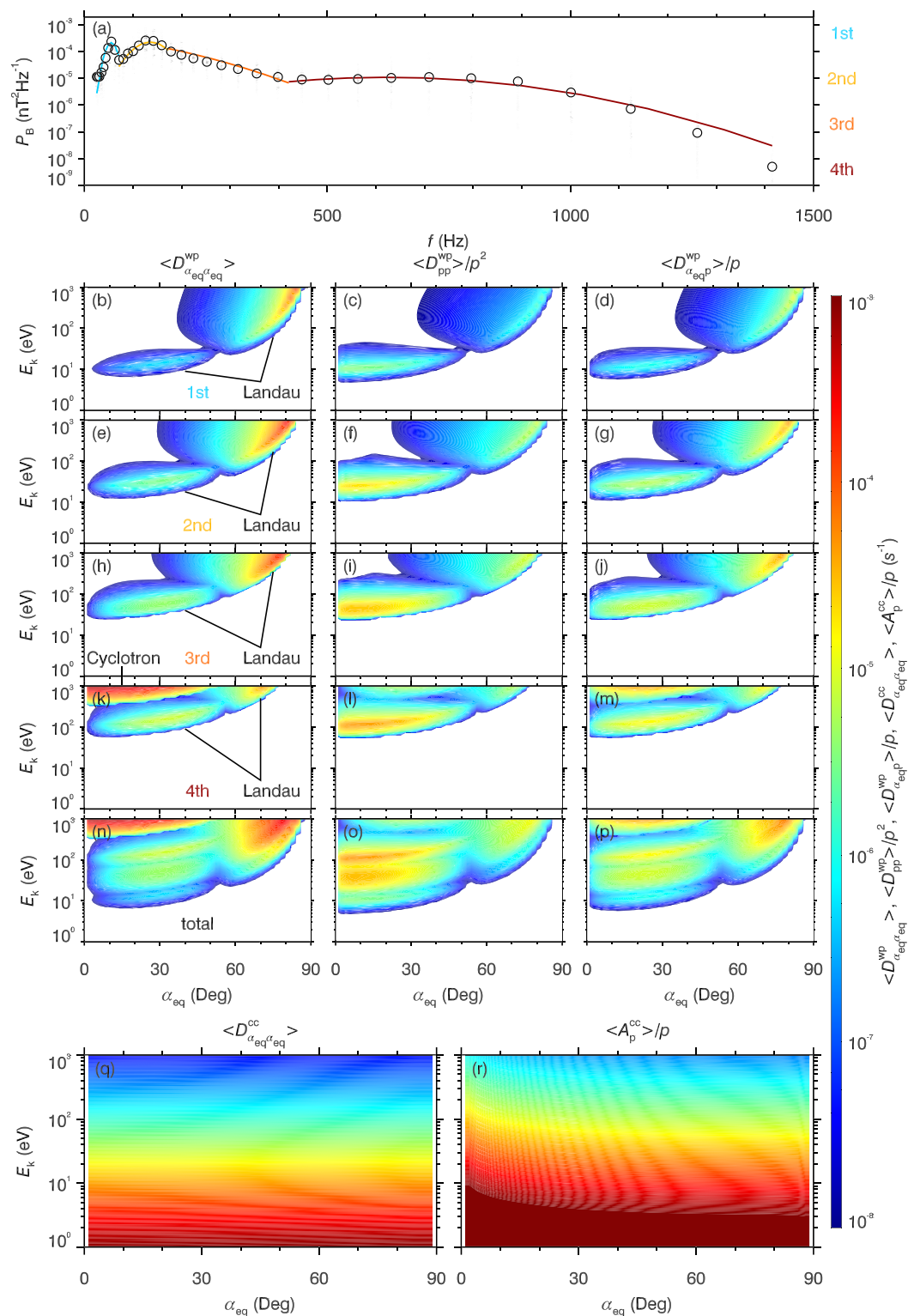


**Figure 2.** Transport rates related to wave-particle interactions and Coulomb collisions: (a) four-segment Gaussian fitting (solid lines) of time-averaged (black circles) hiss wave power spectral densities  $P_B$  (gray circles) observed during TR<sub>1</sub>; (b–p) bounce-averaged diffusion rates (color coded) of the modeled hiss waves  $\langle D_{\alpha_{\text{eq}} \alpha_{\text{eq}}}^{\text{wp}} \rangle$  (left),  $\langle D_{\text{pp}}^{\text{wp}} \rangle / p^2$  (middle) and  $\langle D_{\alpha_{\text{eq}} \alpha_{\text{eq}}}^{\text{wp}} \rangle / p$  (right) for different wave segments and total waves; (q, r) bounce-averaged pitch angle diffusion  $\langle D_{\alpha_{\text{eq}} \alpha_{\text{eq}}}^{\text{cc}} \rangle$  and momentum advection  $\langle A_p^{\text{cc}} \rangle / p$  rates related to the Coulomb collisions.

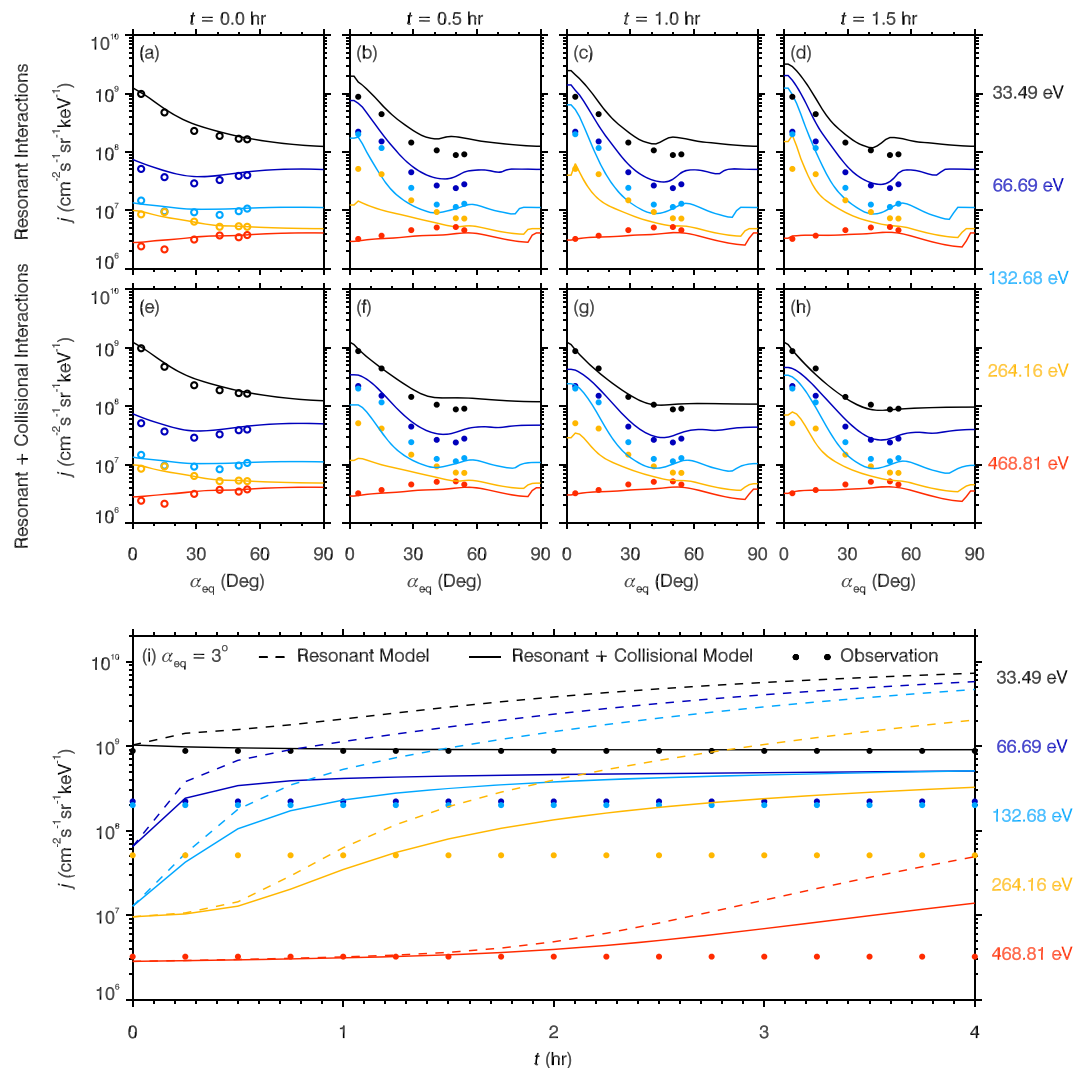


**Figure 3.** Comparison between observed (symbols) and modeled (lines) electron differential fluxes  $j$ : pitch angle-dependent profiles for (a–d) resonant interactions with hiss waves alone and for (e–h) a combination of resonant interactions with hiss waves and Coulomb collisions with background plasma at four moments (indicated); (i) temporal profiles at  $\alpha_{\text{eq}} = 3^\circ$  for resonant interactions alone (dashed) and a combination of resonant interactions and Coulomb collisions (solid). Hollow and solid circles represent the observations during TR<sub>0</sub> and TR<sub>1</sub>, and color helps differentiate among the energy channels.

cold electron density is specified as Equation 4. As shown in Figures 2q and 2r, the collisional transport rates  $\langle D_{\alpha_{\text{eq}} \alpha_{\text{eq}}}^{\text{cc}} \rangle$  and  $\langle A_p^{\text{cc}} \rangle / p$  decrease steeply with the energy increasing. Below several tens of eV, the collisional transport rates are much larger than the wave-driven diffusion rates.

### 3.2. Model-to-Data Comparison

To allow the model-to-data comparison (Figure 3), the observed local pitch angle  $\alpha$  is mapped to the equatorial pitch angle  $\alpha_{\text{eq}}$  through the conservation of magnetic moment, that is,  $\sin^2 \alpha / \sin^2 \alpha_{\text{eq}} = B_o / B_{\text{eq}}$ . Along an arbitrary field line, the ratio  $B_o / B_{\text{eq}}$  between the equatorial and local magnetic field magnitudes is determined by the TS04 geomagnetic model (Tsyganenko & Sitnov, 2005).

The initial electron phase space density is given in the following form

$$F(\alpha_{\text{eq}}, E_k) = \begin{cases} F_o(\alpha_{\text{eq}}, E_k)|_{\text{TR}_0}, & 14 \text{ eV} \leq E_k < 1 \text{ keV}; \\ F_m(E_k) \cdot R_{\alpha_{\text{eq}}}(\alpha_{\text{eq}}), & 1 \text{ eV} < E_k < 14 \text{ eV}. \end{cases} \quad (5)$$

Above 14 eV, the initial condition  $F_o$  is a bicubic spline smooth approximation of the measurements during TR<sub>0</sub>, which had no strong hiss waves but was close to TR<sub>1</sub> both spatially and temporally. These suprathermal electrons of TR<sub>0</sub> may be in a quasi-steady state under the actions of multiple ionospheric and magnetospheric processes (Khazanov & Liemohn, 1995). Below 14 eV, the initial condition is empirically given by a product between an  $\alpha_{eq}$ -dependent factor

$$R_{\alpha_{eq}} = \frac{F_o(\alpha_{eq}, E_k = 14\text{eV})}{F_o(\alpha_{eq} = 90^\circ, E_k = 14\text{eV})} \quad (6)$$

and an isotropic Maxwellian distribution

$$F_m = N_{eq} \left( \frac{m_e}{2\pi E_0} \right)^{\frac{3}{2}} e^{-\frac{E_k}{E_0}} \quad (7)$$

with the ambient cold electron density  $N_{eq} = 78 \text{ cm}^{-3}$ , the thermal energy  $E_0 = 1.7 \text{ eV}$  and the electron rest mass  $m_e$ . In general, the modeled initial electron fluxes peak in the field-aligned direction below 400 eV and gradually transform into the flat distributions above 400 eV (Figures 3a and 3e).

Figures 3b–3d clearly show the gradual wave heating of electrons from lower to higher energies along with time. For the Landau resonance with electrons below 300 eV (Figure 2), the momentum diffusion coefficients peak near  $\alpha_{eq} = 0^\circ$  and the pitch angle diffusion coefficients peak at the moderate pitch angles  $\alpha_{eq} \approx 30^\circ$ . The resulted heating effect is most significant at low pitch angles and declines with the pitch angle increasing. For  $>330 \text{ eV}$  electrons, as the result of the weak momentum diffusion of the Landau resonance but the strong pitch angle diffusion of the cyclotron resonance, no heating effect is observable. At  $t = 1.5 \text{ hr}$ , the hiss-driven resonant diffusion alone has generally reproduced the flux enhancement of 264 eV electrons but overestimated the fluxes of 33–132 eV electrons by up to 10 times (Figure 3d). The addition of Coulomb collisions has caused the suprathermal electrons to deposit their energy partially in the cold plasmaspheric electrons and significantly improved the model-to-data agreement below 200 eV (Figures 3e–3h). Within 1.5 hr, the variations in the fluxes of 33 and 468 eV electrons are ignorable, and the field-aligned fluxes of 66–264 eV electrons increase by 1 order of magnitude or more. This modeling time duration of 1.5 hr is reasonable, as estimated from the available observations in Figure 1. The final sampling time was close to 05:10 UT, and a first-order estimation of the starting time of intense plume hiss waves was 03:30 UT around which Van Allen Probe B encountered the substorm injection front. There were extremely weak waves in the two finger-like plumes before 03:30 UT, and the subsequent measurements in the plumes indicated the emergence of intense hiss waves. As shown in Figure 3i, in contrast to the steadily increasing overestimation of the field-aligned fluxes over time by the model with resonant interactions alone, the addition of Coulomb collisions reduces the temporal growth rates of the field-aligned fluxes and causes these fluxes to saturate at lower levels. These simulations support the idea that the observed energy-dependent enhancement of field-aligned suprathermal electrons could result from the competition between the wave Landau heating and the Coulomb collisional cooling.

#### 4. Discussion

The collisional cooling rates are proportional to the background density  $N_e$  and steeply decrease with energy  $E_k$  increasing (Figure 2r). The Landau heating rates are proportional to the square of wave amplitude  $B_t^2$ , and the Landau heating at higher energies is affected less by the collisional cooling. Figures 4a and 4b show the minimum Landau resonant energy  $E_R$  (Summers et al., 2007) as a function of the equatorial ratio  $f_{pe}/f_{ce}$  of plasma frequency to electron gyrofrequency, the normalized wave frequency  $f/f_{ce}$ , and the wave normal angle  $\psi_B$ .  $E_R$  increases significantly with  $f_{pe}/f_{ce}$  decreasing or  $f/f_{ce}$  increasing but depends less on  $\psi_B$ . In comparison to the plasmaspheric body, the plasmaspheric plume usually has a smaller  $N_e$  but larger  $B_t$  and  $f/f_{ce}$  (Shi et al., 2019; Su et al., 2018a). Hence, the Landau heating of plume hiss waves can prevail over the collisional cooling at relatively high energies, and the enhanced field-aligned suprathermal electrons may deposit their energy, more or less, to the ionospheric plasma.

We compare the field-aligned electron fluxes  $j$  among three representative periods in Figure 4c. As marked in Figure 1, TR<sub>1</sub> and TR<sub>2</sub> with intense hiss waves were inside the plasmaspheric plumes, and TR<sub>3</sub> with moderate hiss waves was inside the plasmaspheric body. In the energy range  $50 \text{ eV} < E_k < 300 \text{ eV}$  where  $\langle D_{pp}^{wp} \rangle / p^2$

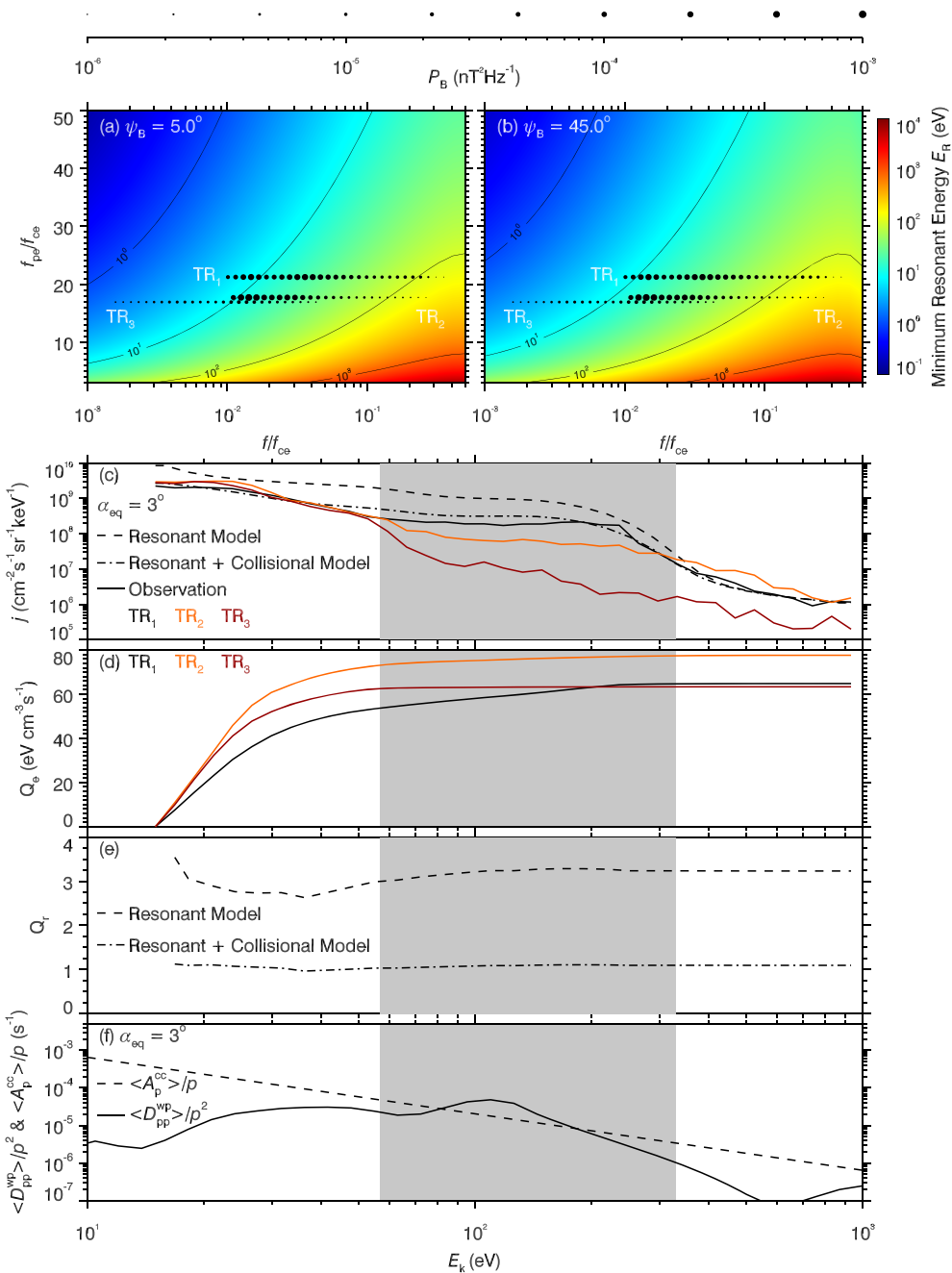


**Figure 4.** Competition between Landau heating and collisional cooling: (a, b) electron minimum Landau resonant energies  $E_R$  (color coded) as functions of the normalized frequency  $f/f_{ce}$  and the equatorial ratio of plasma frequency to electron gyrofrequency  $f_{pe}/f_{ce}$  for whistler mode waves with normal angles  $\psi_B = 5.0^\circ$  (left) and  $45^\circ$  (right), with the overplotted dots marking  $f/f_{ce}$ ,  $f_{pe}/f_{ce}$ , and  $P_B$  (size coded) during three time intervals (indicated); (c) energy-dependent electron fluxes  $j$  at  $\alpha_{eq} = 3^\circ$  observed during three time intervals (color coded), with the overplotted TR<sub>1</sub>'s modeling results (dashed line for resonant interactions alone and dash-dotted line for a combination of resonant interactions and Coulomb collisions) at  $t = 1.5$  hr; (d) energy-dependent electron heating rate  $Q_e$  during three time intervals (color coded); (e) TR<sub>1</sub>'s model-to-data ratio  $Q_r$  of electron heating rate (dashed line for resonant interactions alone and dash-dotted line for a combination of resonant interactions and Coulomb collisions) at  $t = 1.5$  hr; (f) energy dependence of  $\langle D_{pp}^{wp} \rangle / p^2$  (solid line) and  $\langle A_p^{cc} \rangle / p$  (dashed line) at  $\alpha_{eq} = 3^\circ$  for TR<sub>1</sub>. The gray shadow marks the energy range with a significant enhancement in the field-aligned electron fluxes.

is close to or above  $\langle A_p^{cc} \rangle / p$  (Figure 4f), TR<sub>1</sub> and TR<sub>2</sub> had up to 1 order of magnitude larger electron fluxes than TR<sub>3</sub>. TR<sub>3</sub> had the moderate-amplitude ( $B_t < 0.1$  nT), low-frequency ( $f/f_{ce} = 10^{-3}$  to  $10^{-2}$ ) hiss waves but the dense ( $N_e = 10^3$  cm<sup>-3</sup>) background plasma (Figures 1b and 1c), during which the Landau heating effect centering at tens of eV could have been canceled out by the strong Coulomb collisional cooling effect. Because TR<sub>1</sub> and TR<sub>2</sub> had larger wave amplitudes ( $B_t = 0.2$ –0.3 nT) and higher frequencies ( $f/f_{ce} > 10^{-2}$ ), the Landau heating could prevail over the collisional cooling at relatively high energies. Probably because of a shorter duration of wave-particle interactions starting around 03:30 UT, TR<sub>2</sub> had a weaker enhancement in the 50–300 eV electron fluxes than TR<sub>1</sub>.

The ionospheric electron heating rate by field-aligned suprathermal electrons with energies from  $E_s$  to  $E_f$  may be written as (Stamnes & Rees, 1983; Swartz et al., 1971)

$$Q_e(E_s, E_f) = N_e \int_{E_s}^{E_f} \sigma(E_k) I(E_k) dE_k, \quad (8)$$

with the ionospheric electron density  $N_e$ , the stopping cross section  $\sigma(E_k)$ , and the total suprathermal electron flux integrated over solid angle  $I(E_k)$ . In the measurable energy range >14 eV by Van Allen Probes, the stopping cross section  $\sigma(E_k)$  may be approximated as (Swartz et al., 1971; Stamnes & Rees, 1983)

$$\sigma(E_k) = 3.37 \times 10^{-12} E_k^{-0.94} N_e^{-0.03}, \quad (9)$$

with  $\sigma$ ,  $E_k$  and  $N_e$  in units of eV · cm<sup>2</sup>, eV and cm<sup>-3</sup>, respectively. Simply taking the ionospheric density  $N_e = 10^6$  cm<sup>-3</sup>, the total flux  $I = 4\pi \times j(\alpha_{eq} = 3^\circ)$ , and the lower-energy limit  $E_s = 14$  eV, we calculate the ionospheric electron heating rate  $Q_e$  as a function of the upper energy limit in Figure 4d. The total heating rate is sensitive to the <30 eV electron fluxes which are controlled by solar radiation and other local parameters of neutral and charged particles in the ionosphere. For TR<sub>3</sub> in the plasmasphere, >50 eV electrons with a low level of intensity appear to be ignorable to the total heating rate. In contrast, the enhancement of >50 eV electrons causes the ionospheric heating rate to increase by nearly 30% for TR<sub>1</sub> in the plume. The realistic ionospheric electron heating rate can be reproduced only when the model takes into account the two competing processes (Figure 4e).

## 5. Summary

Plasmaspheric suprathermal electrons have long been considered to conduct heat flux from the magnetosphere to the ionosphere. In contrast to previous numerous studies about the energy transfer from the ring current ions to the plasmaspheric field-aligned suprathermal electrons, we here examine whether the whistler mode hiss waves growing from the substorm-injected electron instability can heat the field-aligned suprathermal electrons. Because the plasmaspheric plume usually has a smaller plasma density but a larger hiss wave amplitude and a larger normalized wave frequency than the plasmaspheric body, the effective energy transfer from the ring current electrons through the plasmaspheric field-aligned suprathermal electrons to the ionospheric plasma is more likely to occur in the plasmaspheric plume. The quasi-linear simulation taking into account both Landau heating by the hiss waves and collisional cooling with the background plasma can well reproduce the observed energy-dependent enhancements of suprathermal electron fluxes. Below 50 eV, the collisional cooling counteracts largely the wave Landau heating. As the energy increases, the collisional cooling rates decrease steeply. Around 200 eV, the Landau heating causes the field-aligned suprathermal electron fluxes to increase by 1 order of magnitude or above on a time scale of 1.5 hr. Above 400 eV, the cyclotron resonance of hiss waves arises and contributes little to the electron enhancement. For the ionospheric electron heating rate driven by the measurable >14 eV suprathermal electrons, the enhancement of field-aligned >50 eV electrons resulting from the competition between plume hiss wave Landau heating and Coulomb collisional cooling may introduce a 30% additional contribution. Although this letter is limited to a case study, the enhancement of suprathermal electrons related to plume hiss waves appears to be not rare in the observations of Van Allen Probes (see also Li et al., 2019; Woodroffe et al., 2017). In Figures S2 and S3, we have shown two additional events to support the generality of the obtained results. Further work needs to be done to establish whether and then how the ionospheric plasma responds to the intense plume hiss waves excited by the substorm-injected energetic electrons in the magnetosphere.

## Data Availability Statement

Van Allen Probes data are available from the following websites (<http://emfisis.physics.uiowa.edu/Flight/> and [http://www.rbsp-ect.lanl.gov/data\\_pub/](http://www.rbsp-ect.lanl.gov/data_pub/)). Geomagnetic indices are available from this website (<http://wdc.kugi.kyoto-u.ac.jp>).

## Acknowledgments

We acknowledge EMFISIS and ECT teams for the use of Van Allen Probes data. This work was supported by the Strategic Priority Research Program of Chinese Academy of Sciences Grant XDB 41000000, the National Natural Science Foundation of China Grants 41774170 and 41631071, the Chinese Academy of Sciences Grants KZCX2-EW-QN510 and KZZD-EW-01-4, the CAS Key Research Program of Frontier Sciences Grant QYZDB-SSW-DQC015, the National Key Basic Research Special Foundation of China Grant 2011CB811403, the National Postdoctoral Program for Innovative Talents Grant BX20190310, the China Postdoctoral Science Foundation Grant 2019M662171, and the Fundamental Research Funds for the Central Universities WK2080000005.

## References

- Agapitov, O., Mourenas, D., Artemyev, A., Mozer, F. S., Bonnell, J. W., Angelopoulos, V., et al. (2018). Spatial extent and temporal correlation of chorus and hiss: Statistical results from multipoint THEMIS observations. *Journal of Geophysical Research: Space Physics*, 123, 8317–8330. <https://doi.org/10.1029/2018JA025725>
- Albert, J. M. (2010). Diffusion by one wave and by many waves. *Journal of Geophysical Research*, 115, A00F05. <https://doi.org/10.1029/2009JA014732>
- Blake, J. B., Carranza, P. A., Claudepierre, S. G., Clemons, J. H., Crain, W. R., Dotan, Y., et al. (2013). The magnetic electron ion spectrometer (MagEIS) instruments aboard the radiation belt storm probes (RBSP) spacecraft. *Space Science Reviews*, 179, 383–421. <https://doi.org/10.1007/s11214-013-9991-8>
- Bortnik, J., Thorne, R. M., & Meredith, N. P. (2008). The unexpected origin of plasmaspheric hiss from discrete chorus emissions. *Nature*, 452, 62–66. <https://doi.org/10.1038/nature06741>
- Brace, L. H., Chappell, C. R., Chandler, M. O., Comfort, R. H., & Horwitz, J. L. (1988). F region electron temperature signatures of the plasmapause based on Dynamics Explorer 1 and 2 measurements. *Journal of Geophysical Research*, 93, 1896–1908. <https://doi.org/10.1029/JA093iA03p01896>
- Chen, L., Bortnik, J., Thorne, R. M., Horne, R. B., & Jordanova, V. K. (2009). Three-dimensional ray tracing of VLF waves in a magnetospheric environment containing a plasmaspheric plume. *Geophysical Research Letters*, 36, L22101. <https://doi.org/10.1029/2009GL040451>
- Cole, K. D. (1965). Stable auroral red arcs, sinks for energy of  $D_{st}$  main phase. *Journal of Geophysical Research*, 70, 1689–1706. <https://doi.org/10.1029/JZ070i007p01689>
- Cornwall, J. M., Coroniti, F. V., & Thorne, R. M. (1971). Unified theory of SAR arc formation at the plasmapause. *Journal of Geophysical Research*, 76, 4428. <https://doi.org/10.1029/JA076i019p04428>
- Denton, R. E., Goldstein, J., Menietti, J. D., & Young, S. L. (2002). Magnetospheric electron density model inferred from polar plasma wave data. *Journal of Geophysical Research*, 107, 1386. <https://doi.org/10.1029/2001JA009136>
- Erlandson, R. E., Aggson, T. L., Hogey, W. R., & Slavin, J. A. (1993). Simultaneous observations of subauroral electron temperature enhancements and electromagnetic ion cyclotron waves. *Geophysical Research Letters*, 20, 1723–1726. <https://doi.org/10.1029/93GL01975>
- Fok, M. C., Kozyra, J. U., Nagy, A. F., & Cravens, T. E. (1991). Lifetime of ring current particles due to Coulomb collisions in the plasmasphere. *Journal of Geophysical Research*, 96, 7861–7867. <https://doi.org/10.1029/90JA02620>
- Foster, J. C., Buonsanto, M. J., Mendillo, M., Nottingham, D., Rich, F. J., & Denig, W. (1994). Coordinated stable auroral red arc observations: Relationship to plasma convection. *Journal of Geophysical Research*, 99, 11,429–11,440. <https://doi.org/10.1029/93JA03140>
- Funsten, H. O., Skoug, R. M., Guthrie, A. A., MacDonald, E. A., Baldonado, J. R., Harper, R. W., et al. (2013). Helium, oxygen, proton, and electron (HOPE) mass spectrometer for the radiation belt storm probes mission. *Space Science Reviews*, 179, 423–484. <https://doi.org/10.1007/s11214-013-9968-7>
- Green, J. L., Brace, L. H., Waite, J. H., Chappell, C. R., Chandler, M. O., Doupnik, J. R., et al. (1986). Observations of ionospheric magnetospheric coupling—DE and Chatanika coincidences. *Journal of Geophysical Research*, 91, 5803–5815. <https://doi.org/10.1029/JA091iA05p05803>
- Gurgiolo, C., Sandel, B. R., Perez, J. D., Mitchell, D. G., Pollock, C. J., & Larsen, B. A. (2005). Overlap of the plasmasphere and ring current: Relation to subauroral ionospheric heating. *Journal of Geophysical Research*, 110, A12217. <https://doi.org/10.1029/2004JA010986>
- Hanson, W. B. (1964). Dynamic diffusion processes in the exosphere. In E. Thrane (Ed.), *Electron density distribution in ionosphere and exosphere* (pp. 351).
- Hasegawa, A., & Mima, K. (1978). Anomalous transport produced by kinetic Alfvén wave turbulence. *Journal of Geophysical Research*, 83, 1117–1123. <https://doi.org/10.1029/JA083iA03p01117>
- Horne, R. B., & Thorne, R. M. (1993). On the preferred source location for the convective amplification of ion cyclotron waves. *Journal of Geophysical Research*, 98, 9233–9247. <https://doi.org/10.1029/92JA02972>
- Horne, R. B., Thorne, R. M., Glauert, S. A., Albert, J. M., Meredith, N. P., & Anderson, R. R. (2005). Timescale for radiation belt electron acceleration by whistler mode chorus waves. *Journal of Geophysical Research*, 110, A03225. <https://doi.org/10.1029/2004JA010811>
- Horwitz, J. L., Brace, L. H., Comfort, R. H., & Chappell, C. R. (1986). Dual-spacecraft measurements of plasmasphere-ionosphere coupling. *Journal of Geophysical Research*, 91, 11,203–11,216. <https://doi.org/10.1029/JA091iA10p11203>
- Jordanova, V. K., Kistler, L. M., Kozyra, J. U., Khazanov, G. V., & Nagy, A. F. (1996). Collisional losses of ring current ions. *Journal of Geophysical Research*, 101, 111–126. <https://doi.org/10.1029/95JA02000>
- Khazanov, G. V., Gombosi, T. I., Nagy, A. F., & Koen, M. A. (1992). Analysis of the ionosphere-plasmasphere transport of superthermal electrons. I - Transport in the plasmasphere. *Journal of Geophysical Research*, 97, 16. <https://doi.org/10.1029/92JA00319>
- Khazanov, G. V., & Liemohn, M. W. (1995). Nonsteady state ionosphere-plasmasphere coupling of superthermal electrons. *Journal of Geophysical Research*, 100, 9669–9682. <https://doi.org/10.1029/95JA00526>
- Khazanov, G. V., Moore, T. E., Liemohn, M. W., Jordanova, V. K., & Fok, M. C. (1996). Global, collisional model of high-energy photoelectrons. *Geophysical Research Letters*, 23(4), 331–334. <https://doi.org/10.1029/96GL00148>
- Kletzing, C. A., Kurth, W. S., Acuna, M., MacDowall, R. J., Torbert, R. B., Averkamp, T., et al. (2013). The electric and magnetic field instrument suite and integrated science (EMFISIS) on RBSP. *Space Science Reviews*, 179, 127–181. <https://doi.org/10.1007/s11214-013-9993-6>
- Kozyra, J. U., Shelley, E. G., Comfort, R. H., Brace, L. H., Cravens, T. E., & Nagy, A. F. (1987). The role of ring current O(+) in the formation of stable auroral red arcs. *Journal of Geophysical Research*, 92, 7487–7502. <https://doi.org/10.1029/JA092iA07p07487>
- Kurth, W. S., Pascuale, S. D., Faden, J. B., Kletzing, C. A., Hospodarsky, G. B., Thaller, S., & Wygant, J. R. (2014). Electron densities inferred from plasma wave spectra obtained by the waves instrument on Van Allen Probes. *Journal of Geophysical Research: Space Physics*, 120, 904–914. <https://doi.org/10.1002/2014JA020857>

- Lemaire, J. F., & Gringauz, K. I. (Eds.) (1998). *The Earth's plasmasphere*. New York: Cambridge University Press. <https://doi.org/10.1007/978-1-4419-1323-4>
- Li, J., Ma, Q., Bortnik, J., Li, W., An, X., Reeves, G. D., et al. (2019). Parallel acceleration of suprathermal electrons caused by whistler-mode hiss waves. *Geophysical Research Letters*, 46, 12,675–12,684. <https://doi.org/10.1029/2019GL085562>
- Li, W., Ma, Q., Thorne, R. M., Bortnik, J., Kletzing, C. A., Kurth, W. S., et al. (2015). Statistical properties of plasmaspheric hiss derived from Van Allen Probes data and their effects on radiation belt electron dynamics. *Journal of Geophysical Research: Space Physics*, 120, 3393–3405. <https://doi.org/10.1002/2015JA021048>
- Liemohn, M. W., Kozyra, J. U., Richards, P. G., Khazanov, G. V., Buonsanto, M. J., & Jordanova, V. K. (2000). Ring current heating of the thermal electrons at solar maximum. *Journal of Geophysical Research*, 105(A12), 27,767–27,776. <https://doi.org/10.1029/2000JA000088>
- Liu, K., Lemons, D. S., Winske, D., & Gary, S. P. (2010). Relativistic electron scattering by electromagnetic ion cyclotron fluctuations: Test particle simulations. *Journal of Geophysical Research*, 115, A04204. <https://doi.org/10.1029/2009JA014807>
- Lyons, L. R., & Thorne, R. M. (1972). Parasitic pitch angle diffusion of radiation belt particles by ion cyclotron waves. *Journal of Geophysical Research*, 77, 5608.
- Lyons, L. R., & Williams, D. J. (1984). *Quantitative aspects of magnetospheric physics*. New York: Springer.
- Meredith, N. P., Horne, R. B., Glauert, S. A., & Anderson, R. R. (2007). Slot region electron loss timescales due to plasmaspheric hiss and lightning-generated whistlers. *Journal of Geophysical Research*, 112, A08214. <https://doi.org/10.1029/2007JA012413>
- Meredith, N. P., Horne, R. B., Kersten, T., Li, W., Sicard, A., & Yearby, K. H. (2018). Global model of plasmaspheric hiss from multiple satellite observations. *Journal of Geophysical Research: Space Physics*, 123, 4526–4541. <https://doi.org/10.1029/2018JA025226>
- Meredith, N. P., Horne, R. B., Thorne, R. M., Summers, D., & Anderson, R. R. (2004). Substorm dependence of plasmaspheric hiss. *Journal of Geophysical Research*, 109, A06209. <https://doi.org/10.1029/2004JA010387>
- Ni, B., Li, W., Thorne, R. M., Bortnik, J., Ma, Q., Chen, L., et al. (2014). Resonant scattering of energetic electrons by unusual low-frequency hiss. *Geophysical Research Letters*, 41, 1854–1861. <https://doi.org/10.1002/2014GL059389>
- Omura, Y., Nakamura, S., Kletzing, C. A., Summers, D., & Hikishima, M. (2015). Nonlinear wave growth theory of coherent hiss emissions in the plasmasphere. *Journal of Geophysical Research: Space Physics*, 120, 7642–7657. <https://doi.org/10.1002/2015JA021520>
- Santolík, O., Parrot, M., & Lefèuvre, F. (2003). Singular value decomposition methods for wave propagation analysis. *Radio Science*, 38, 1010. <https://doi.org/10.1029/2000RS002523>
- Santolík, O., Pickett, J. S., Gurnett, D. A., Menietti, J. D., Tsurutani, B. T., & Verkhoglyadova, O. (2010). Survey of Poynting flux of whistler mode chorus in the outer zone. *Journal of Geophysical Research*, 115, A00F13. <https://doi.org/10.1029/2009JA014925>
- Santolík, O., Pickett, J. S., Gurnett, D. A., & Storey, L. R. O. (2002). Magnetic component of narrowband ion cyclotron waves in the auroral zone. *Journal of Geophysical Research*, 107, 1444. <https://doi.org/10.1029/2001JA000146>
- Schulz, M., & Lanzerotti, L. J. (1974). *Particle diffusion in the radiation belts*, *Physics and Chemistry in Space* (Vol. 7). New York: Springer. <https://doi.org/10.1007/978-3-642-65657-0>
- Schunk, R. W., & Nagy, A. (2009). *Ionospheres: Physics, plasma physics, and chemistry*, *Cambridge Atmospheric and Space Science Series* (2nd ed.). Cambridge: Cambridge University Press. <https://doi.org/10.1017/CBO9780511635342>
- Shi, R., Li, W., Ma, Q., Green, A., Kletzing, C. A., Kurth, W. S., et al. (2019). Properties of whistler mode waves in earth's plasmasphere and plumes. *Journal of Geophysical Research: Space Physics*, 124, 1035–1051. <https://doi.org/10.1029/2018JA026041>
- Spence, H. E., Reeves, G. D., Baker, D. N., Blake, J. B., Bolton, M., Bourdarie, S., et al. (2013). Science goals and overview of the radiation belt storm probes (RBSP) energetic particle, composition, and thermal plasma (ECT) suite on nasa's Van Allen Probes mission. *Space Science Reviews*, 179, 311–336. <https://doi.org/10.1007/s11214-013-0007-5>
- Stamnes, K., & Rees, M. H. (1983). Heating of thermal ionospheric electrons by suprathermal electrons. *Geophysical Research Letters*, 10(4), 309–312. <https://doi.org/10.1029/GL010i004p00309>
- Su, Z., Liu, N., Zheng, H., Wang, Y., & Wang, S. (2018a). Large-amplitude extremely low frequency hiss waves in plasmaspheric plumes. *Geophysical Research Letters*, 45, 565–577. <https://doi.org/10.1002/2017GL076754>
- Su, Z., Liu, N., Zheng, H., Wang, Y., & Wang, S. (2018b). Multipoint observations of nightside plasmaspheric hiss generated by substorm-injected electrons. *Geophysical Research Letters*, 45, 10,921–10,932. <https://doi.org/10.1029/2018GL079927>
- Su, Z., Xiao, F., Zheng, H., & Wang, S. (2010). STEERB: A three-dimensional code for storm-time evolution of electron radiation belt. *Journal of Geophysical Research*, 115, A09208. <https://doi.org/10.1029/2009JA015210>
- Su, Z., Zhu, H., Xiao, F., Zheng, H., Shen, C., Wang, Y., & Wang, S. (2012). Bounce-averaged advection and diffusion coefficients for monochromatic electromagnetic ion cyclotron wave: Comparison between test-particle and quasi-linear models. *Journal of Geophysical Research*, 117, A09222. <https://doi.org/10.1029/2012JA017917>
- Su, Z., Zhu, H., Xiao, F., Zheng, H., Zhang, M., Liu, Y. C. M., et al. (2014). Latitudinal dependence of nonlinear interaction between electromagnetic ion cyclotron wave and terrestrial ring current ions. *Physics of Plasmas*, 21(5), 052310. <https://doi.org/10.1063/1.4880036>
- Summers, D., Ni, B., & Meredith, N. P. (2007). Timescales for radiation belt electron acceleration and loss due to resonant wave-particle interactions: 1. Theory. *Journal of Geophysical Research*, 112, A04206. <https://doi.org/10.1029/2006JA011801>
- Summers, D., Ni, B., Meredith, N. P., Horne, R. B., Thorne, R. M., Moldwin, M. B., & Anderson, R. R. (2008). Electron scattering by whistler-mode ELF hiss in plasmaspheric plumes. *Journal of Geophysical Research*, 113, A04219. <https://doi.org/10.1029/2007JA012678>
- Summers, D., Omura, Y., Nakamura, S., & Kletzing, C. A. (2014). Fine structure of plasmaspheric hiss. *Journal of Geophysical Research: Space Physics*, 119, 9134–9149. <https://doi.org/10.1002/2014JA020437>
- Swartz, W. E., Nisbet, J. S., & Green, A. E. S. (1971). Analytic expression for the energy-transfer rate from photoelectrons to thermal-electrons. *Journal of Geophysical Research*, 76(34), 8425–8426. <https://doi.org/10.1029/JA076i034p08425>
- Tao, X., Bortnik, J., Albert, J. M., Liu, K., & Thorne, R. M. (2011). Comparison of quasilinear diffusion coefficients for parallel propagating whistler mode waves with test particle simulations. *Geophysical Research Letters*, 380, L06105. <https://doi.org/10.1029/2011GL046787>
- Thorne, R. M., Church, S. R., & Gorney, D. J. (1979). On the origin of plasmaspheric hiss—The importance of wave propagation and the plasmapause. *Journal of Geophysical Research*, 84, 5241–5247. <https://doi.org/10.1029/JA084iA09p05241>
- Thorne, R. M., & Horne, R. B. (1992). The contribution of ion-cyclotron waves to electron heating and SAR-arc excitation near the storm-time plasmapause. *Geophysical Research Letters*, 19, 417–420. <https://doi.org/10.1029/92GL00089>
- Tsurutani, B. T., Falkowski, B. J., Pickett, J. S., Santolík, O., & Lakhina, G. S. (2015). Plasmaspheric hiss properties: Observations from Polar. *Journal of Geophysical Research: Space Physics*, 120, 414–431. <https://doi.org/10.1002/2014JA020518>
- Tsyganenko, N. A., & Sitnov, M. I. (2005). Modeling the dynamics of the inner magnetosphere during strong geomagnetic storms. *Journal of Geophysical Research*, 110, A03208. <https://doi.org/10.1029/2004JA010798>

- Woodroffe, J. R., Jordanova, V. K., Funsten, H. O., Streltsov, A. V., Bengtson, M. T., Kletzing, C. A., et al. (2017). Van Allen Probes observations of structured whistler mode activity and coincident electron Landau acceleration inside a remnant plasmaspheric plume. *Journal of Geophysical Research: Space Physics*, 122, 3073–3086. <https://doi.org/10.1002/2015JA022219>
- Xiao, F., Su, Z., Zheng, H., & Wang, S. (2009). Modeling of outer radiation belt electrons by multidimensional diffusion process. *Journal of Geophysical Research*, 114, A03201. <https://doi.org/10.1029/2008JA013580>
- Yuan, Z., Xiong, Y., Huang, S., Deng, X., Pang, Y., Zhou, M., et al. (2014). Cold electron heating by EMIC waves in the plasmaspheric plume with observations of the Cluster satellite. *Geophysical Research Letters*, 41, 1830–1837. <https://doi.org/10.1002/2014GL059241>
- Zhang, W., Ni, B., Huang, H., Summers, D., Fu, S., Xiang, Z., et al. (2019). Statistical properties of hiss in plasmaspheric plumes and associated scattering losses of radiation belt electrons. *Geophysical Research Letters*, 46, 5670–5680. <https://doi.org/10.1029/2018GL081863>
- Zhou, Q., Xiao, F., Yang, C., He, Y., & Tang, L. (2013). Observation and modeling of magnetospheric cold electron heating by electromagnetic ion cyclotron waves. *Journal of Geophysical Research: Space Physics*, 118, 6907–6914. <https://doi.org/10.1002/2013JA019263>